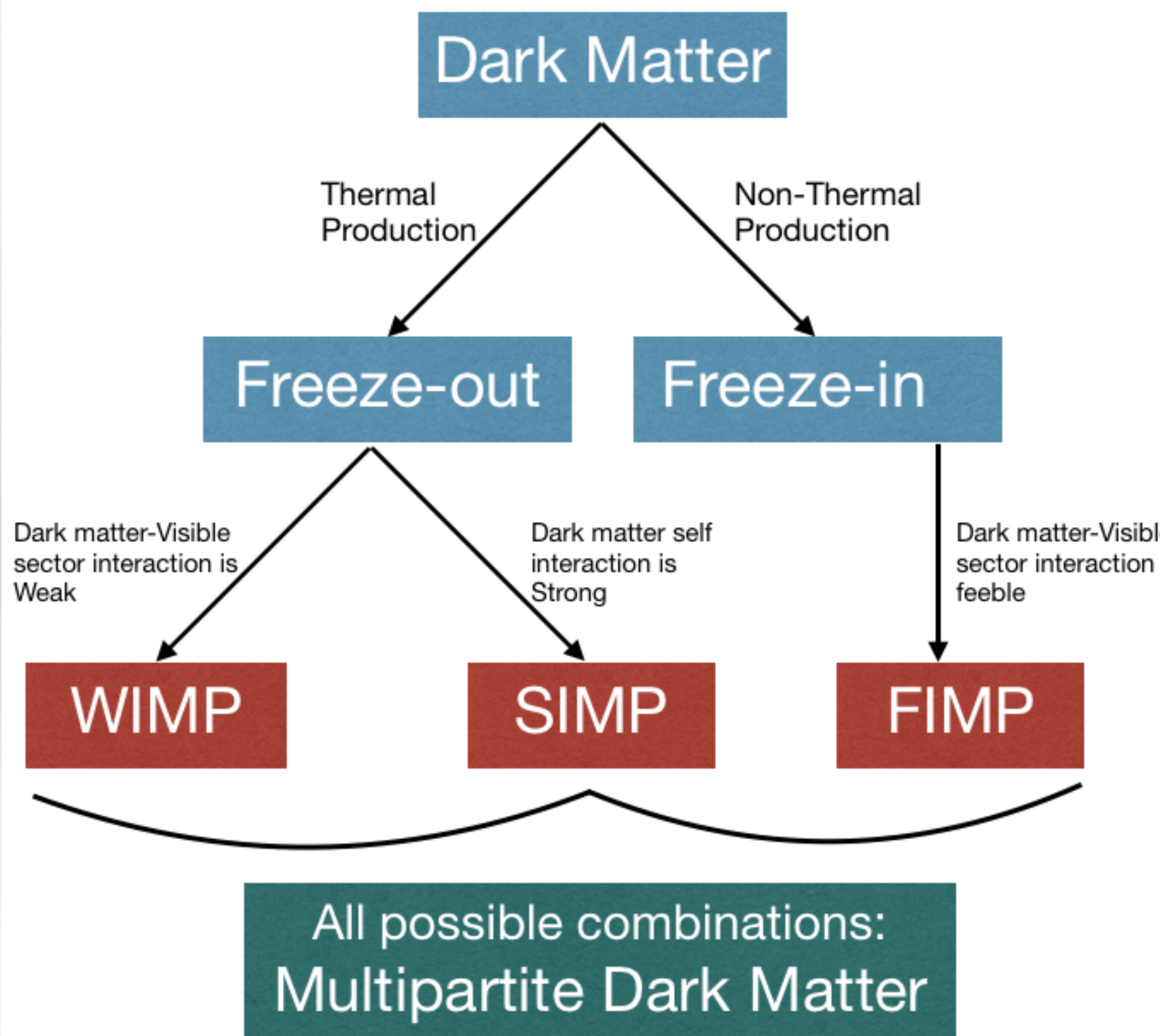


PASCOS 2022, Max Planck Heidelberg, 25/07/22

Features of Multipartite Dark Matter at Collider

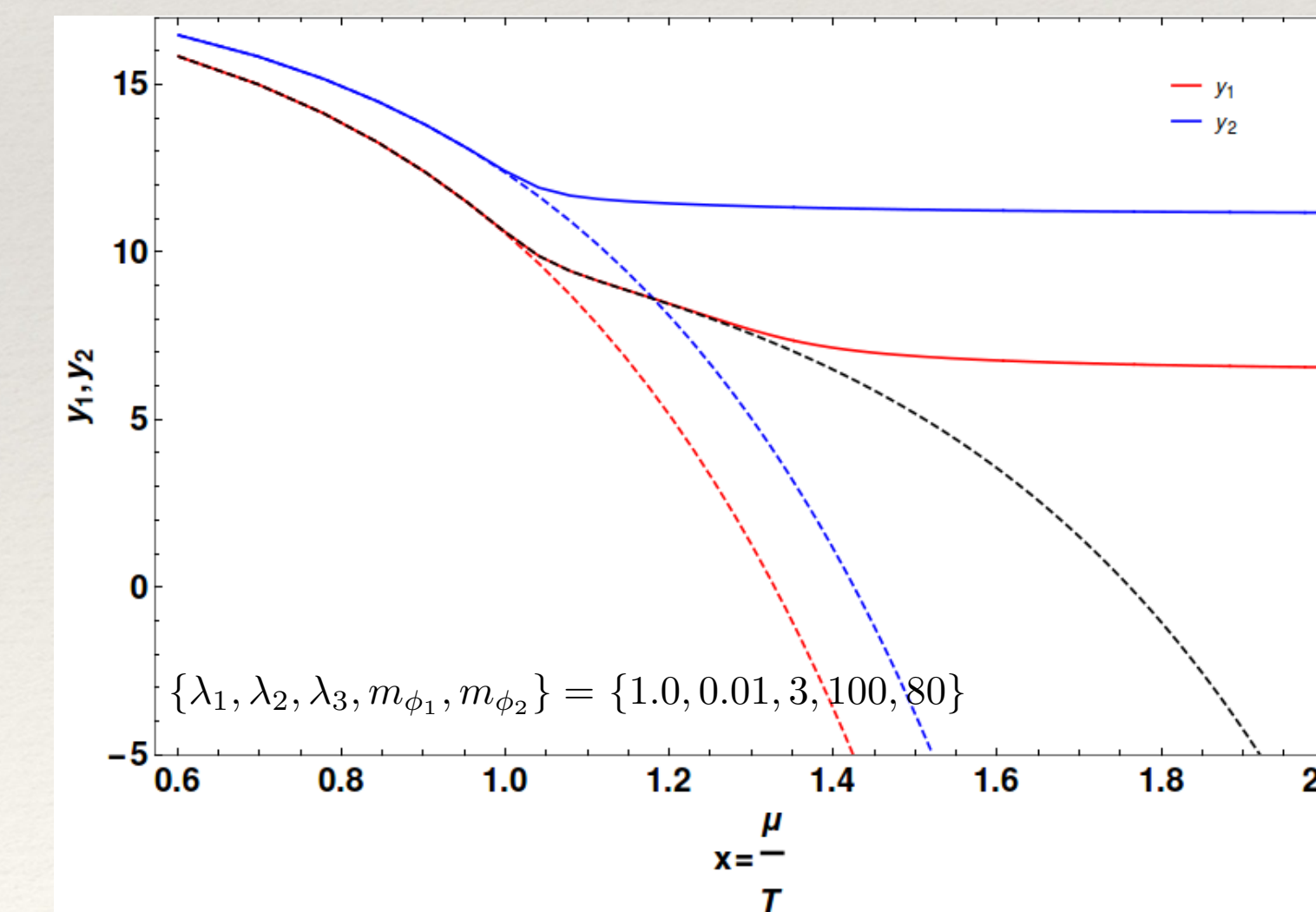
Subhaditya Bhattacharya
IIT Guwahati

Multipartite Dark matter models



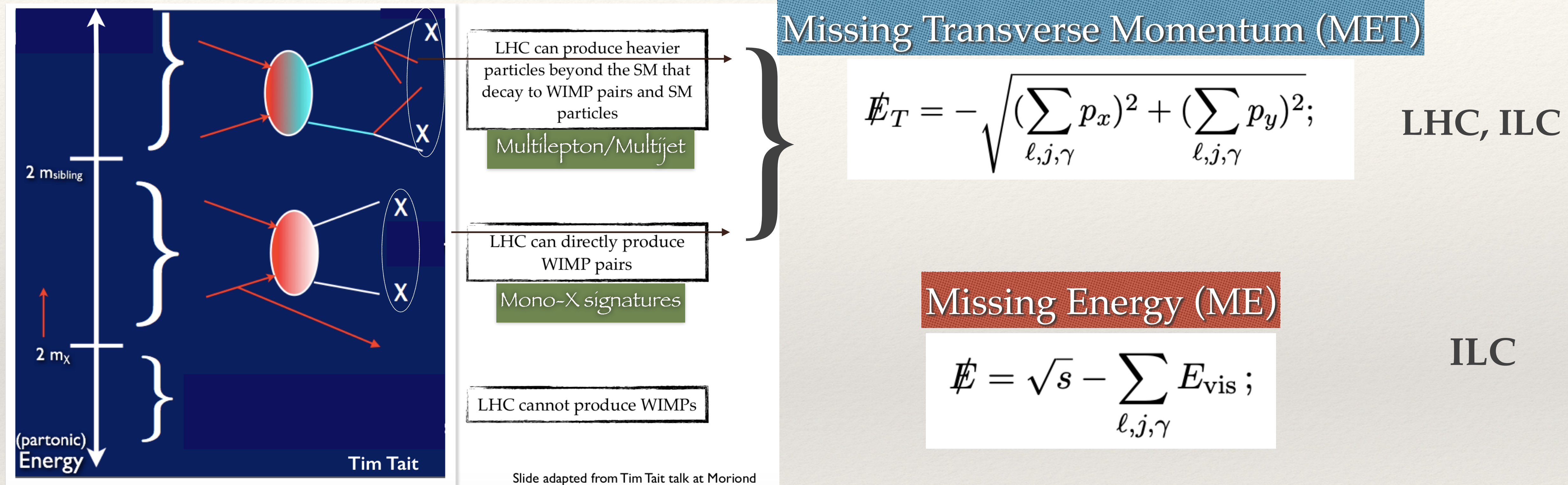
- Coupled Boltzmann Equations to determine relic contribution
- Conversions between dark matter components (WIMP-WIMP)
- Modified freeze-out (WIMP-WIMP)
- Modified direct search cross-section (WIMP-WIMP)
- Larger allowed parameter space

$$\Omega_T h^2 = \Omega_1 h^2 + \Omega_2 h^2 \simeq 0.1199 \pm 0.0022$$



$$\sigma_{eff}^i = \frac{\Omega^i}{\Omega_{tot}} \sigma_{DM-N}$$

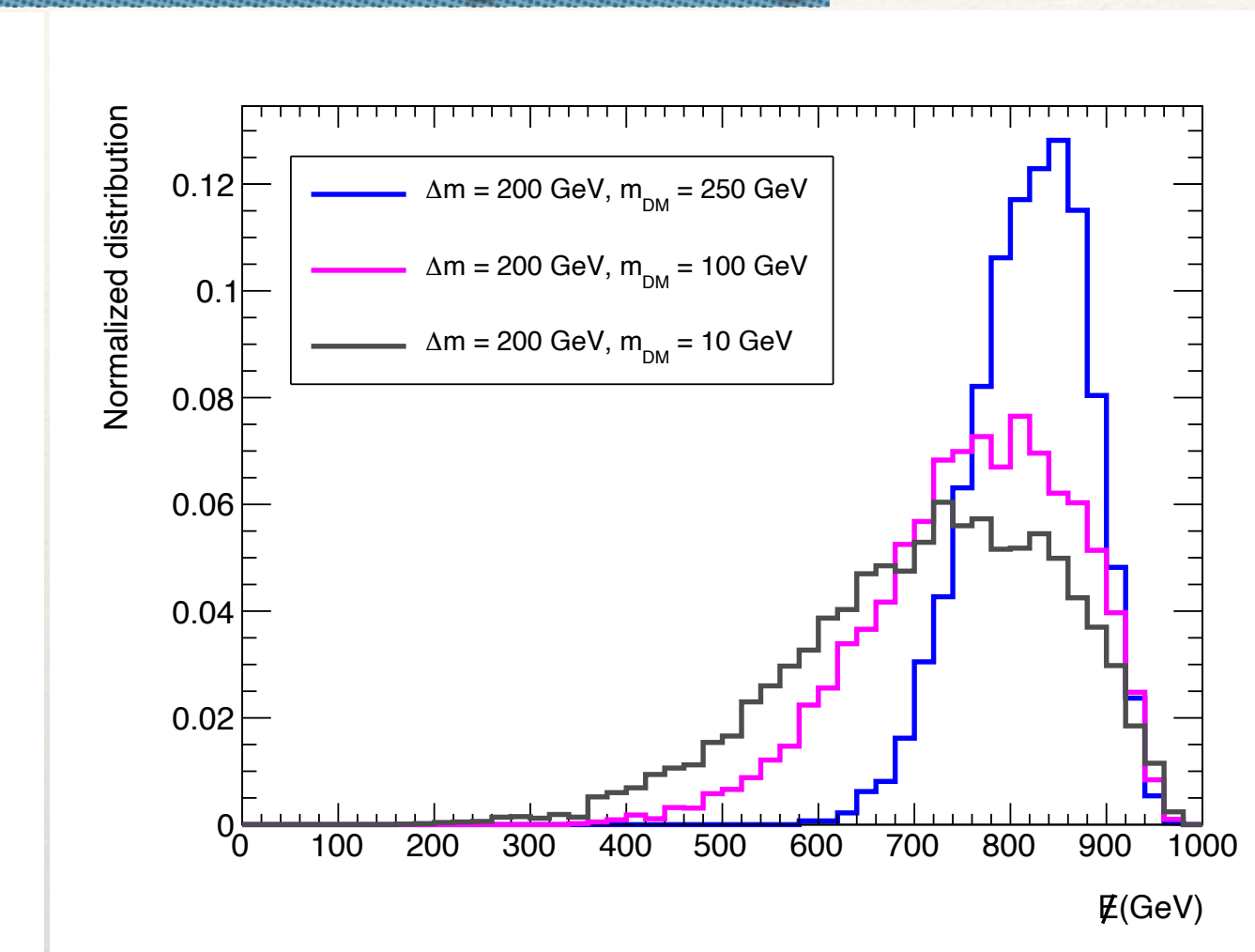
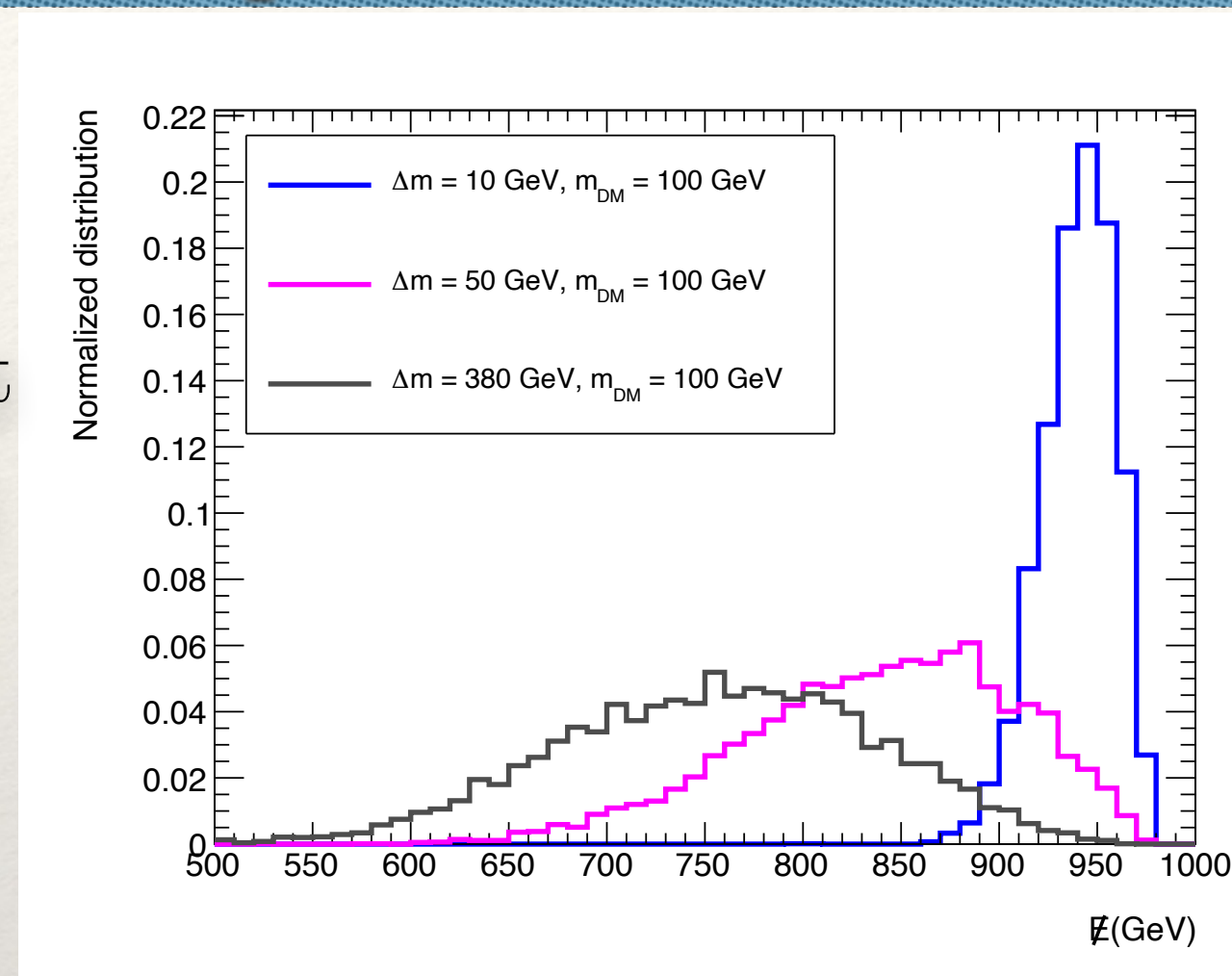
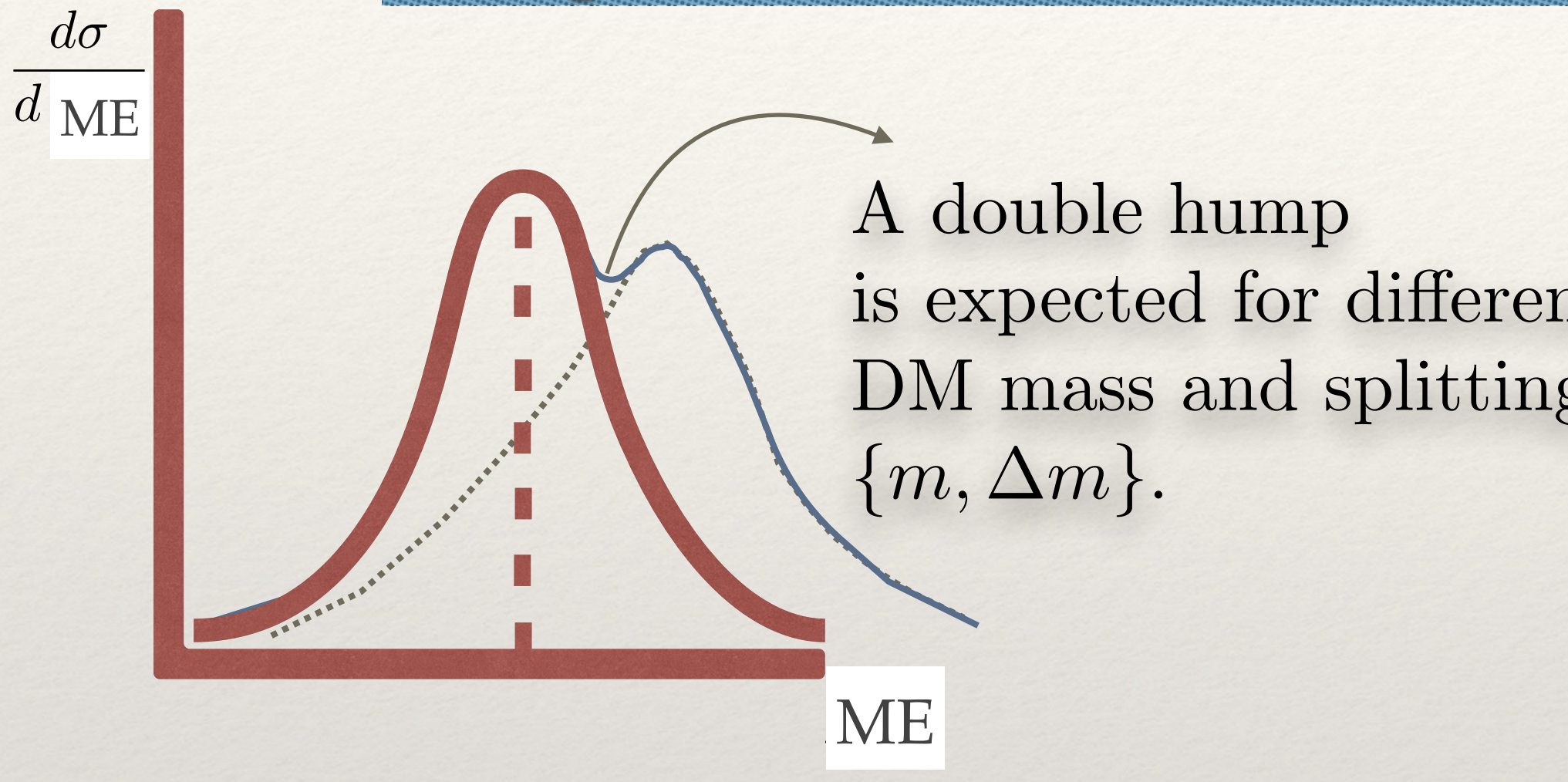
Collider Signal of Dark Matter



- Due to beam polarisation and longitudinal degrees of freedom, ILC is more useful than LHC.
- Due large number of variables, multilepton signals from cascade turn more useful than mono-X signal.

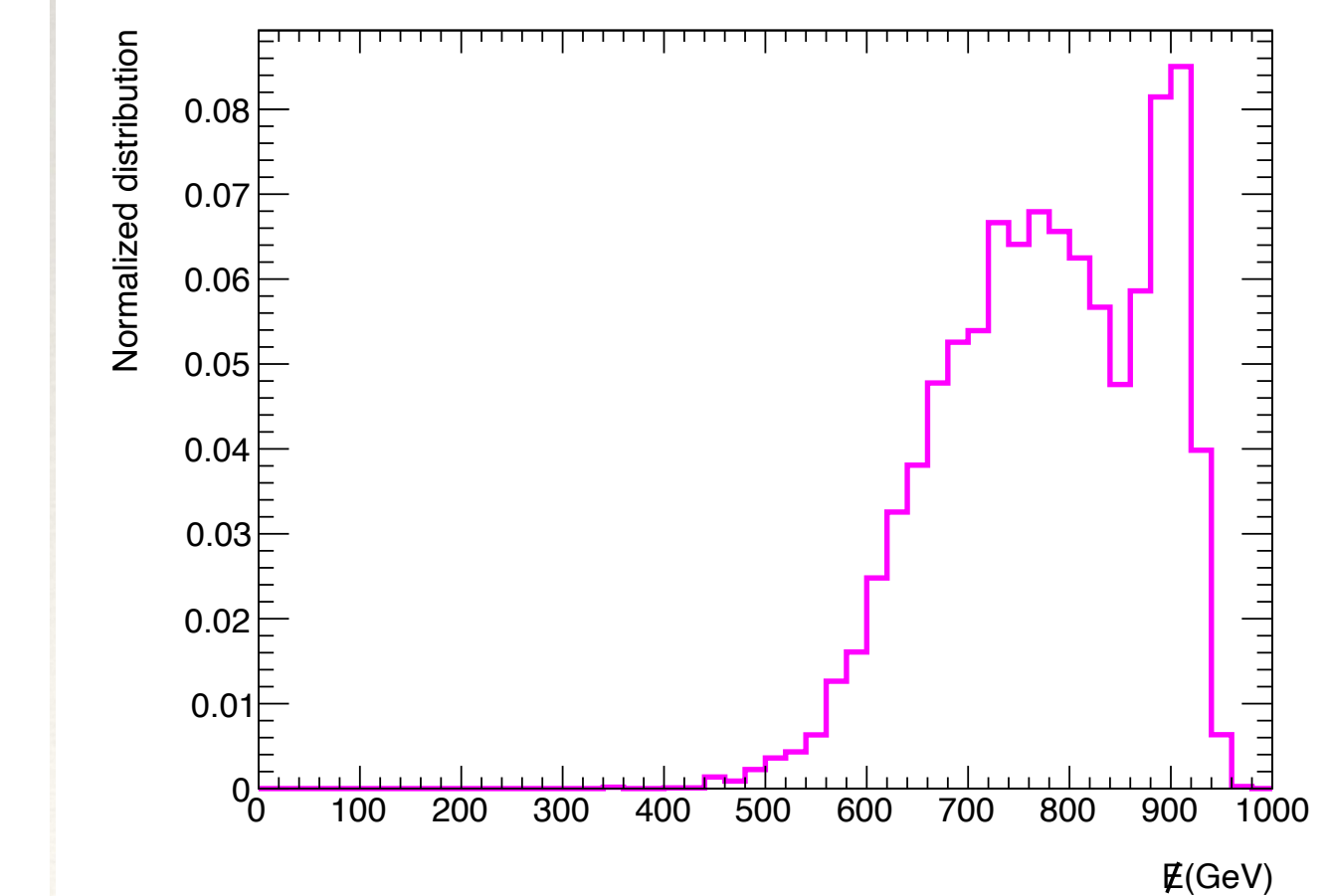
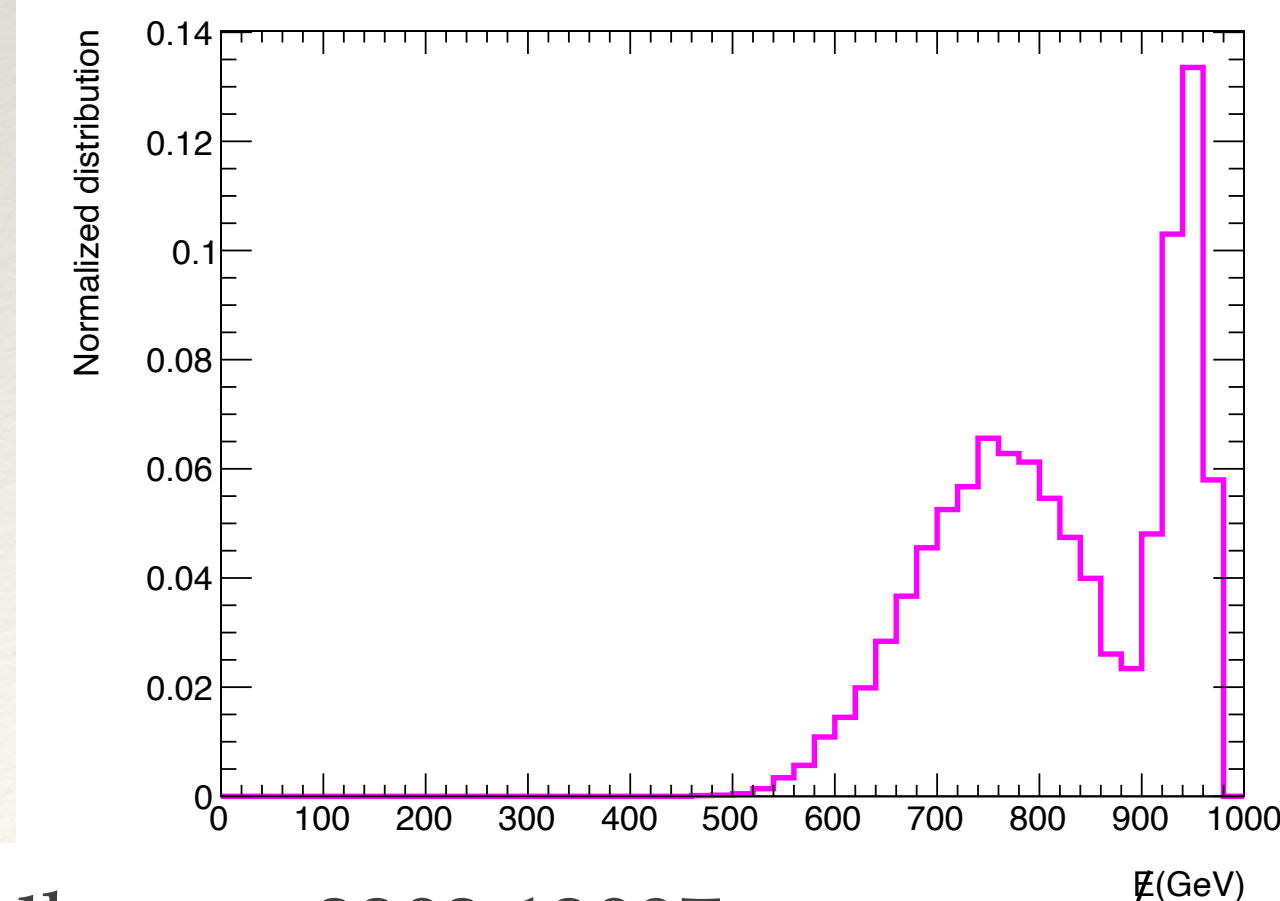
Collider signal of two component DM

The peak of the ME distribution depends on both DM mass and splitting



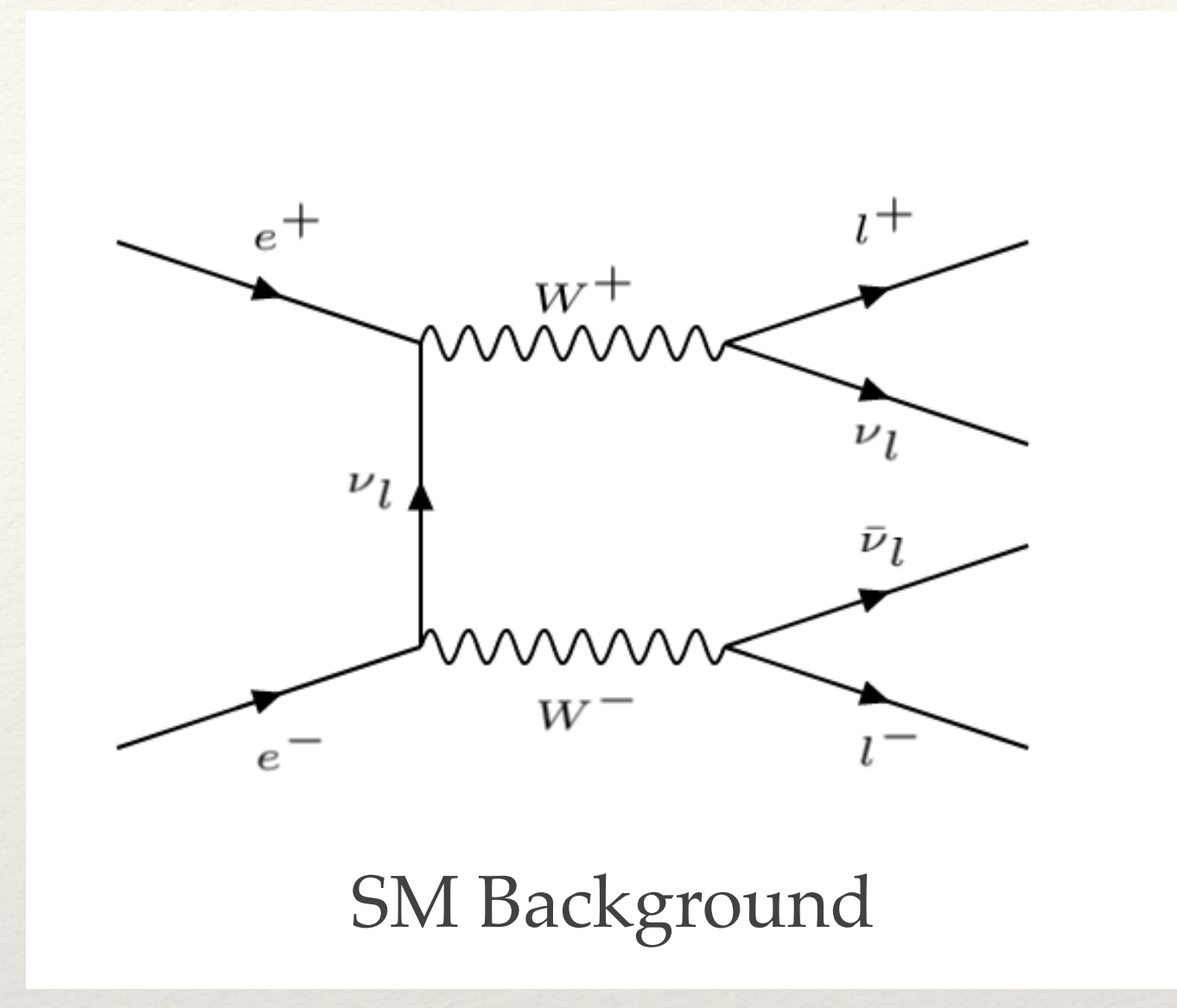
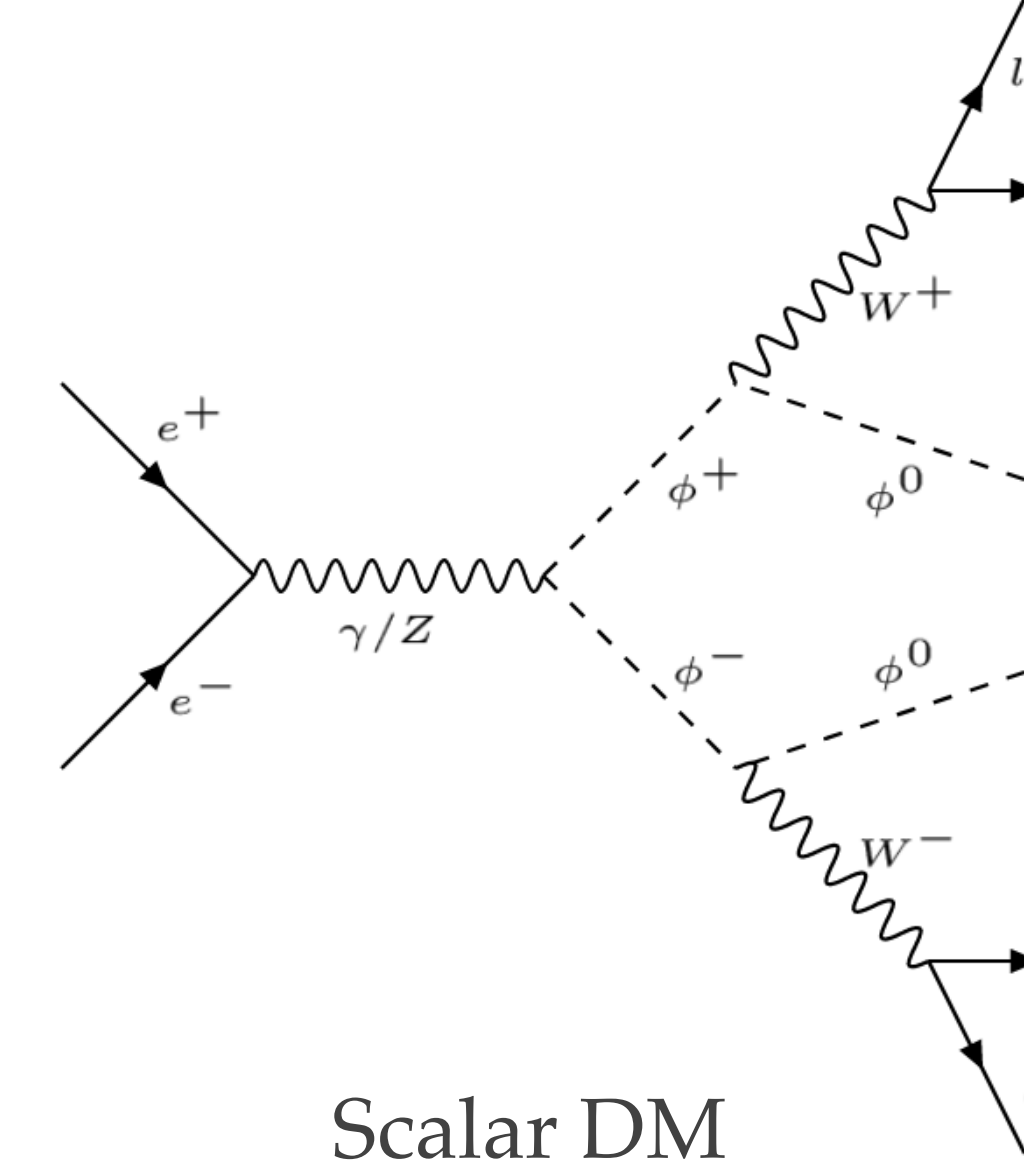
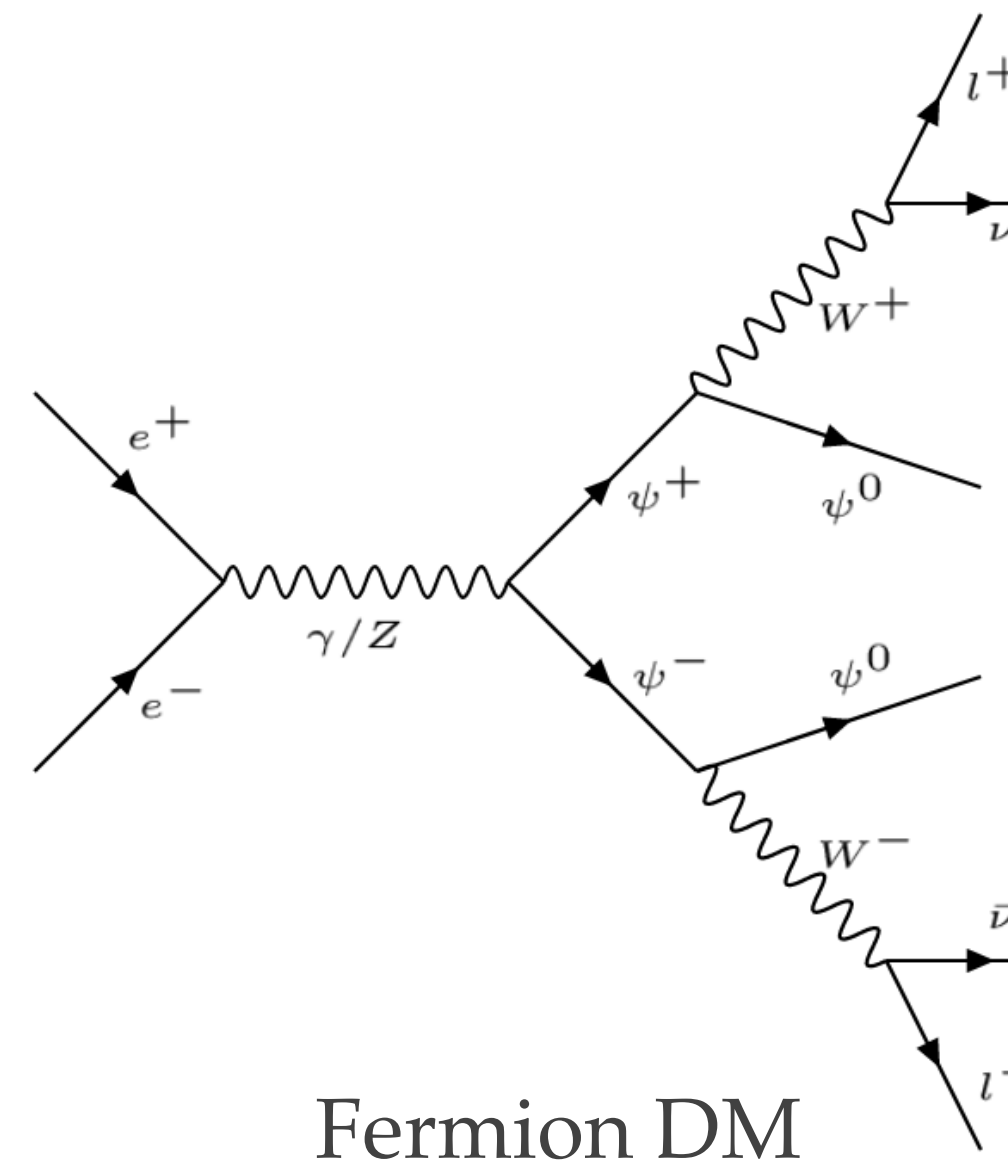
Two peaks in ME/MET can be identified as signal of two component DM

ME works better than MET as it is sensitive to DM mass

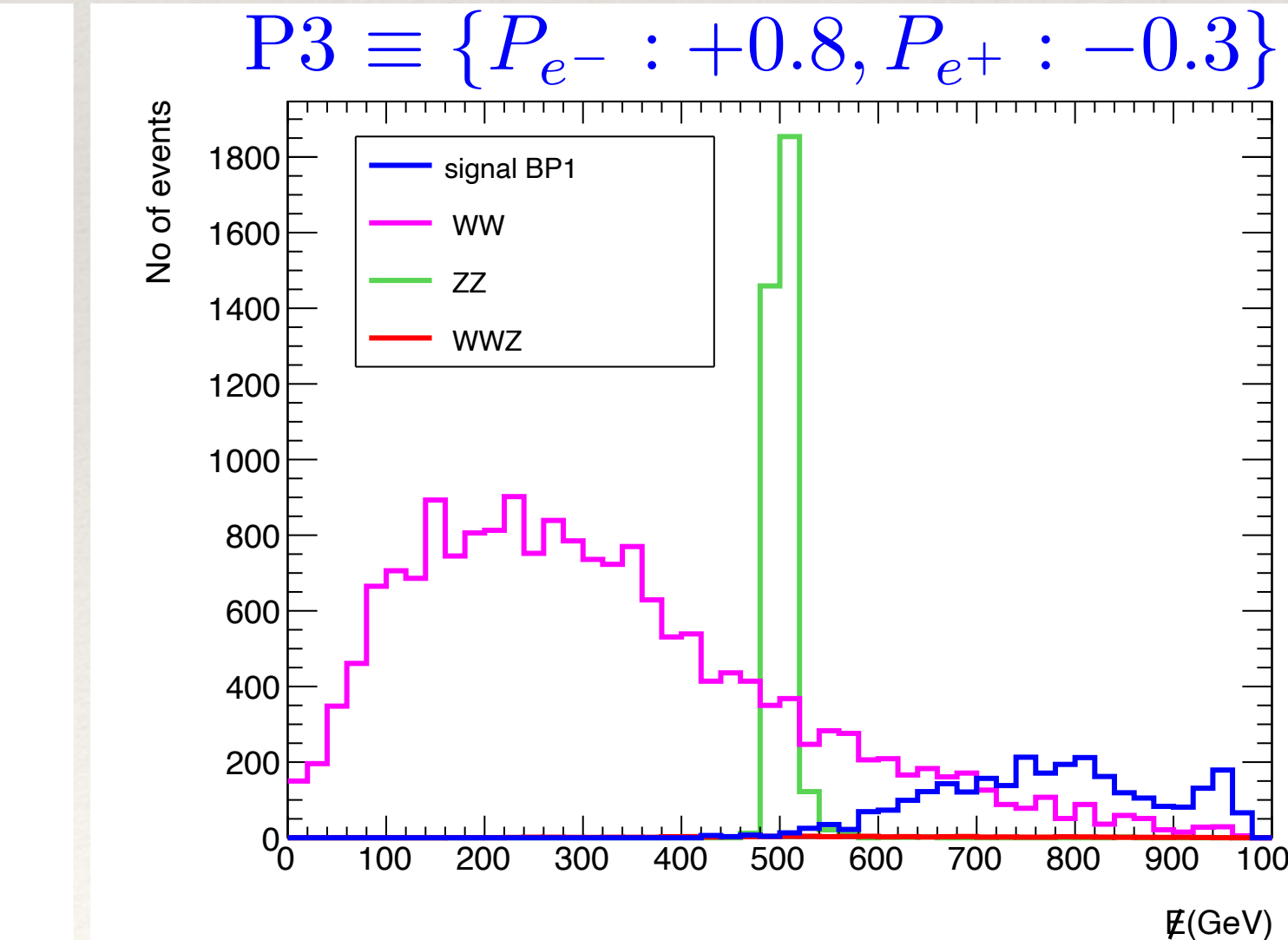
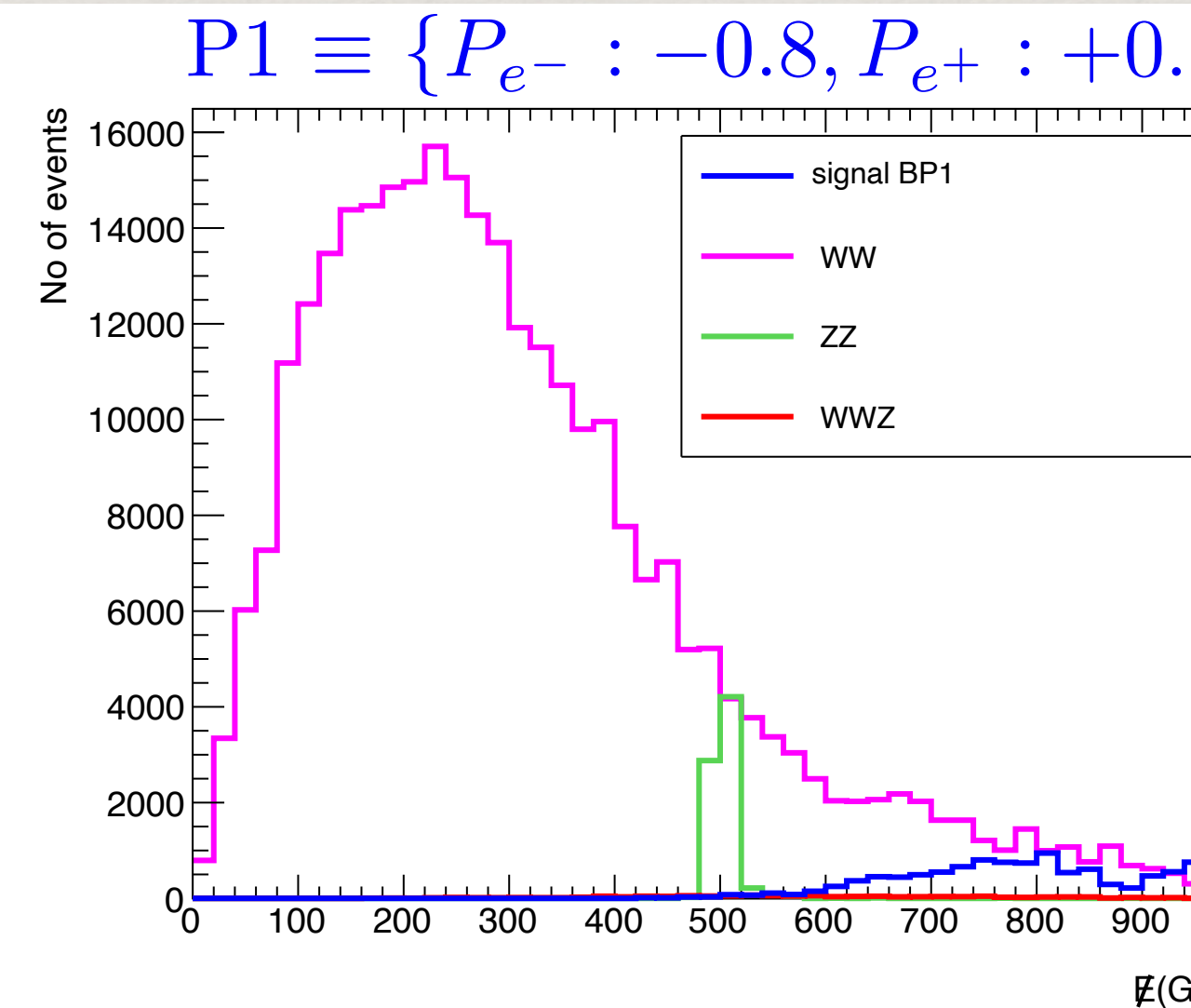


Signal plus background and polarisation

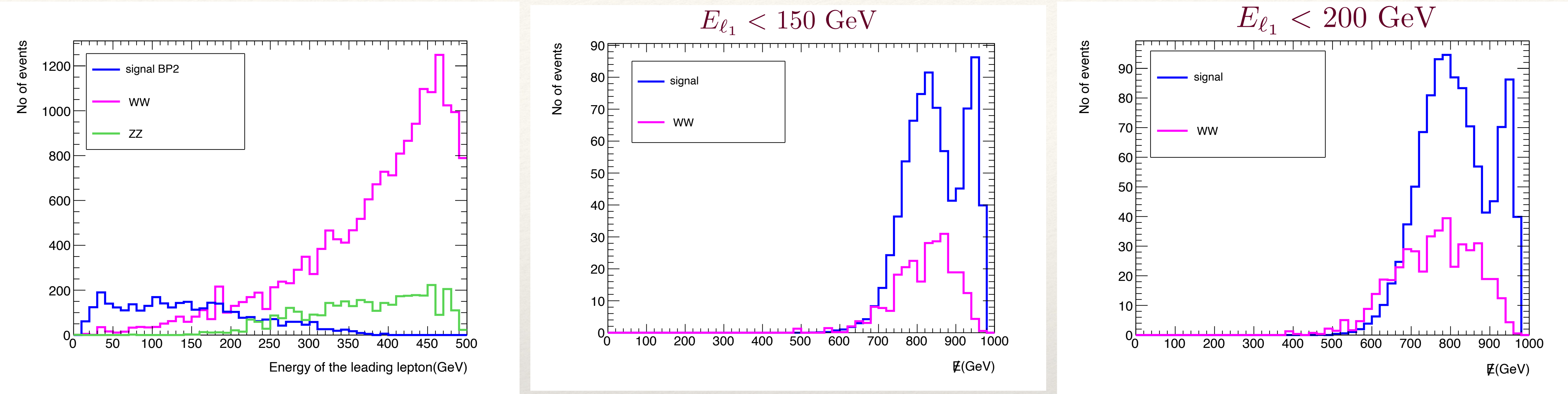
Hadronically quiet
opposite sign dilepton
 $\ell^+ \ell^- + 0j + \text{ME}$



Right polarised electron
and left polarised
positron beam helps in
reducing background



Lepton Energy Cut

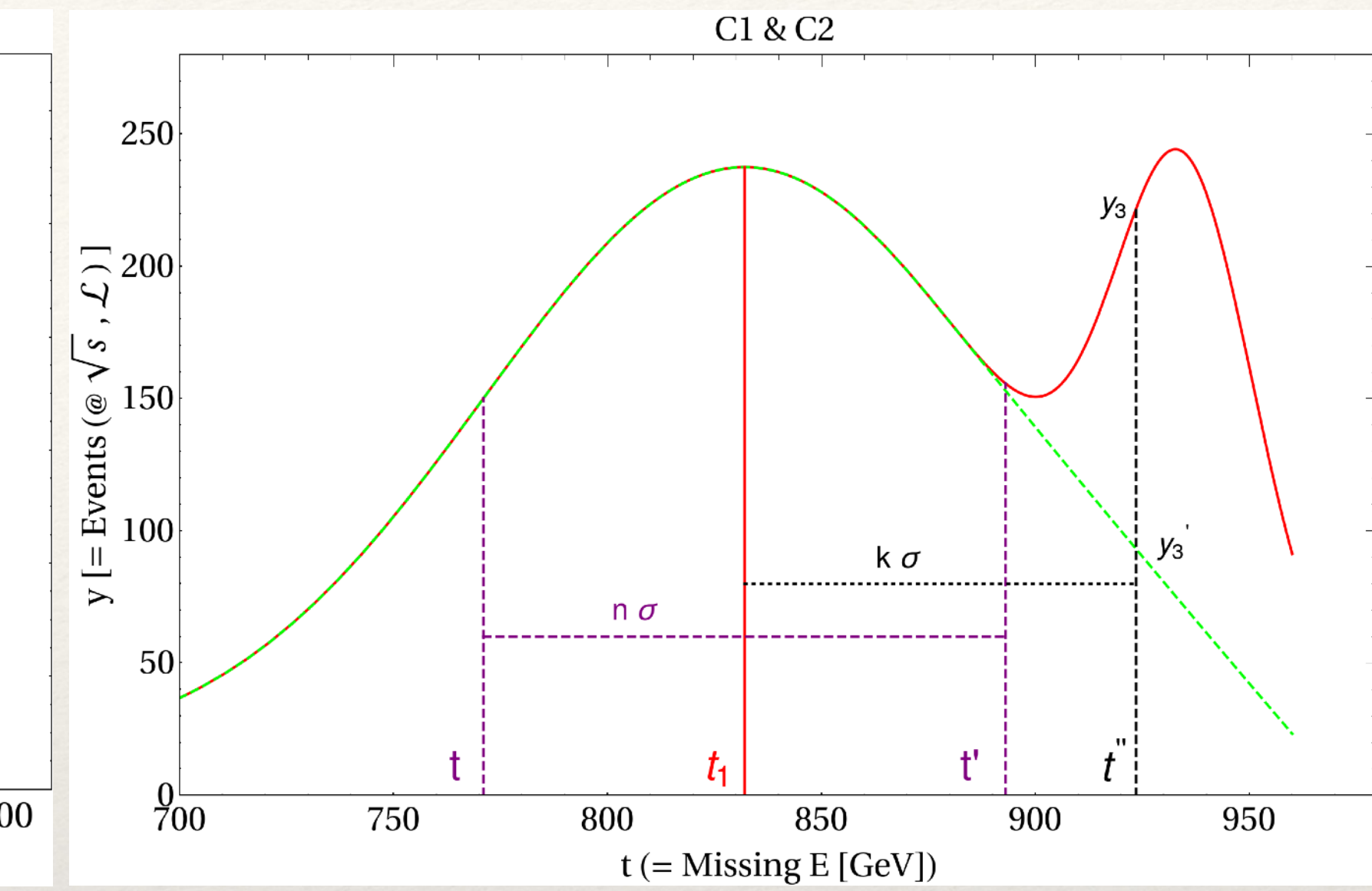
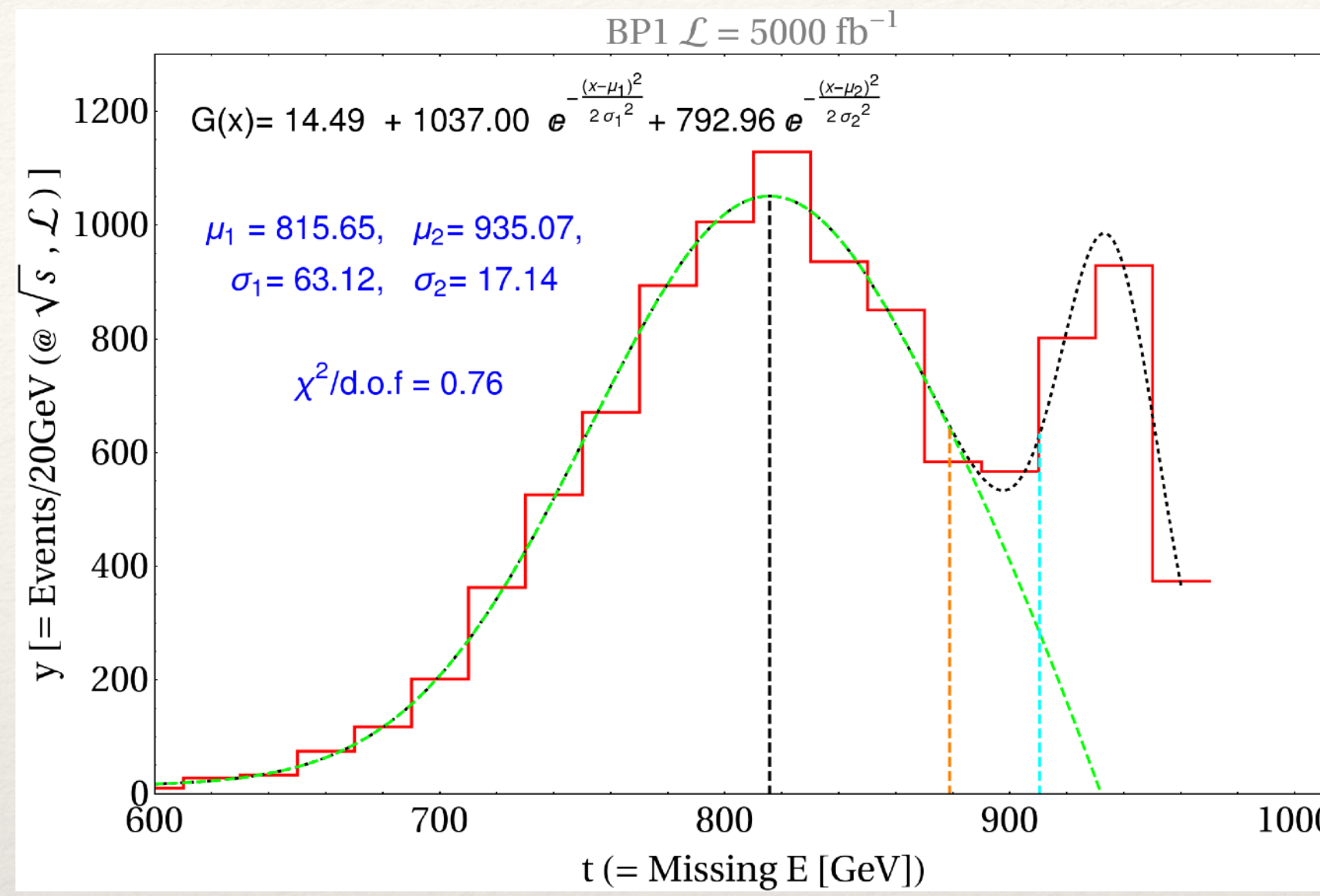


- Lepton energy distribution is complementary to ME distribution.
- A judicious cut on Lepton energy not only reduces the background, but also helps to highlight first peak by aligning it to the first signal peak.

Conditions for segregating the peaks

Gaussian fitting

$$\begin{aligned} G(x) &= G_1(x) + G_2(x) + \mathcal{B} \\ &= A_1 e^{-\frac{(x-\mu_1)^2}{2\sigma_1^2}} + A_2 e^{-\frac{(x-\mu_2)^2}{2\sigma_2^2}} + \mathcal{B}. \end{aligned}$$

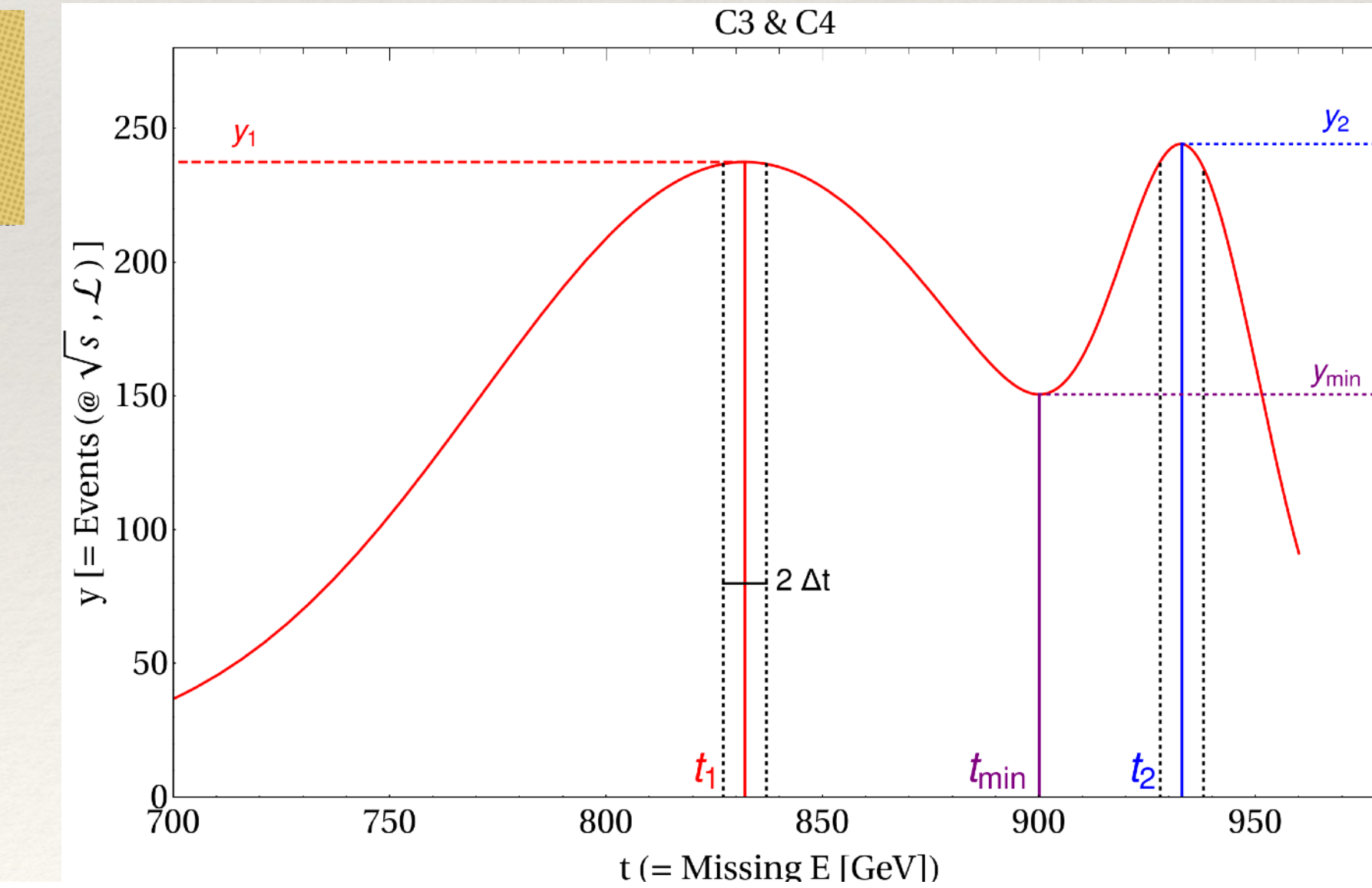


$$C1 : \Delta N_1 = \int_t^{t_1} y dt, \quad \Delta N_2 = \int_{t_1}^{t'} y dt; \quad R_{C1} = \frac{|\Delta N_2 - \Delta N_1|}{\sqrt{\Delta N_1}} \rightarrow R_{C1} > 2.$$

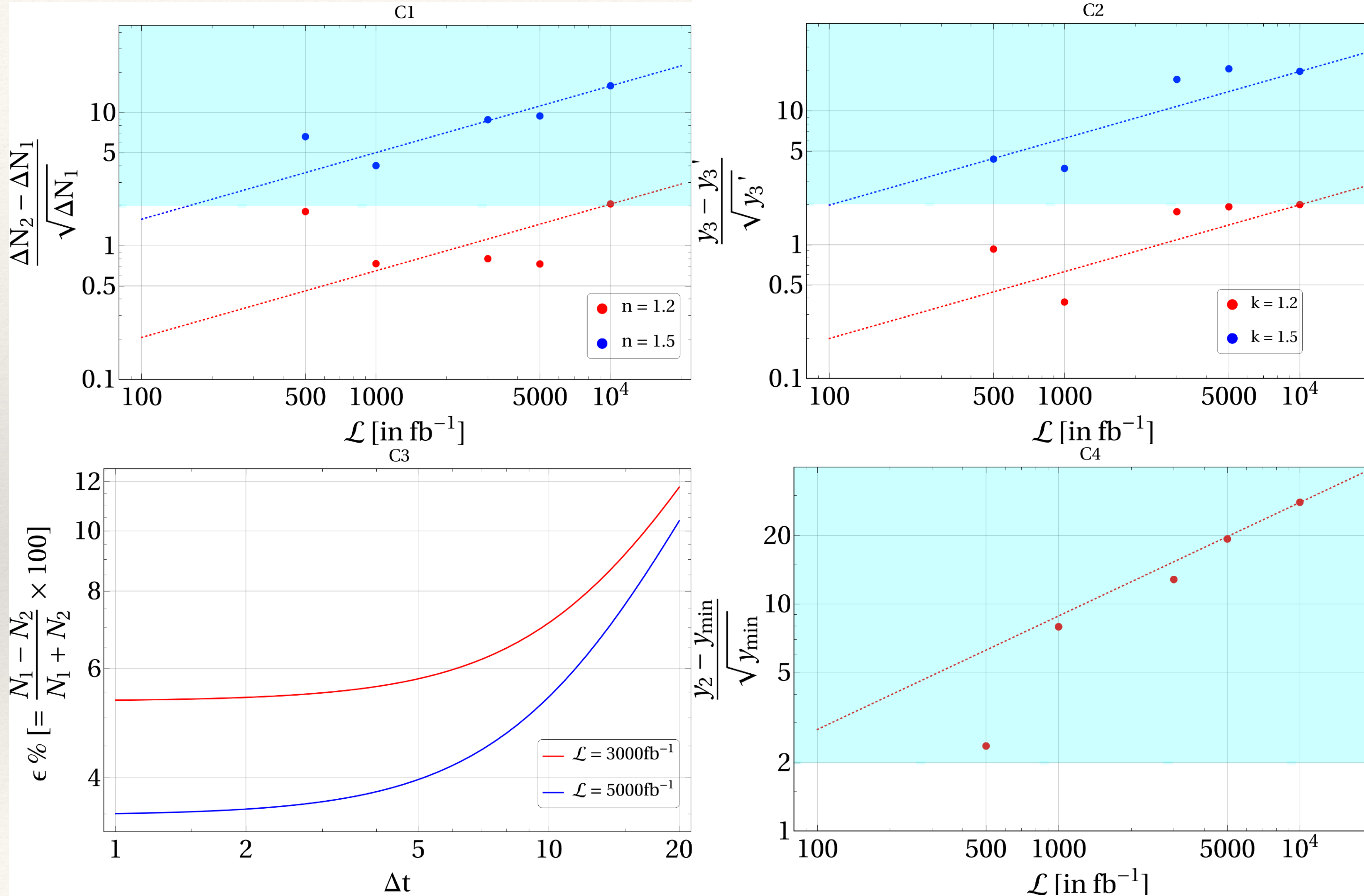
$$C2 : R_{C2} = \frac{y(t'') - y'(t'')}{\sqrt{y'(t'')}} \equiv \frac{y_3 - y'_3}{\sqrt{y'_3}}; \rightarrow R_{C2} > 2$$

$$C3 : R_{C3} = \frac{\int_{t_1-\Delta t}^{t_1+\Delta t} y dt - \int_{t_2-\Delta t}^{t_2+\Delta t} y dt}{\int_{t_1-\Delta t}^{t_1+\Delta t} y dt + \int_{t_2-\Delta t}^{t_2+\Delta t} y dt} \xrightarrow{\{\Delta t \rightarrow 0\}} \frac{y_1 - y_2}{y_1 + y_2}.$$

$$C4 : R_{C4} = \frac{y(t_2) - y(t_{\min})}{\sqrt{y(t_{\min})}} \equiv \frac{y_2 - y_{\min}}{\sqrt{y_{\min}}} \rightarrow R_{C4} > 2.$$



Conditions in terms of Luminosity



- The dots are simulated points.
- The lines are drawn by scaling with luminosity
- The sky blue region depicts 2 or more sigma statistical fluctuations.

Summary and Conclusions

- ★ Two dark sectors producing DM via cascade decay can yield two humps in the ME/MET spectra; ME does better than MET; thus ILC is a better machine explore such possibilities.
- ★ The separation of the peaks depend on m , Δm ; while the height also depend on them via production cross-section. Both are crucially controlled by DM constraints.
- ★ SM background can play foul, where beam polarisation at ILC and lepton energy cut for 2-lepton final state as studied, comes handy.
- ★ The distinction criteria are sensitive to the lepton energy cut for the chosen final state. If the cut is too stringent, the two-peak nature is lost, if the cut is relaxed, the second peak becomes insignificant compared to the first, requiring an optimisation.
- ★ Conditions C1, C2, C3, C4 involving R_{C1} , R_{C2} , R_{C3} and R_{C4} variables respectively, can successfully distinguish double peak behaviour in the ME spectrum. Among them, R_{C4} turns out to be the best.
- ★ Large luminosity helps avoiding statistical fluctuation and satisfying the conditions to segregate the peaks.



Thank you

Additional Slides

Model Example: Scalar+Fermion

Fields		$\underbrace{SU(3)_C \otimes SU(2)_L \otimes U(1)_Y}_{\mathcal{Z}_2} \otimes \underbrace{\mathcal{Z}'_2}_{\mathcal{Z}'_2}$				
SDM	$\Phi = \begin{pmatrix} \phi^+ \\ \frac{1}{\sqrt{2}}(\phi^0 + iA^0) \end{pmatrix}$	1	2	1	-	+
FDM	$\Psi_{L,R} = \begin{pmatrix} \psi \\ \psi^- \end{pmatrix}_{L,R}$	1	2	-1	+	-
	χ_R	1	1	0	+	-

$$\mathcal{L} \supset \mathcal{L}^{\text{SDM}} + \mathcal{L}^{\text{FDM}}.$$

$$\mathcal{L}^{\text{SDM}} = \left| \left(\partial^\mu - ig_2 \frac{\sigma^a}{2} W^{a\mu} - ig_1 \frac{Y}{2} B^\mu \right) \Phi \right|^2 - V(\Phi, H);$$

$$V(\Phi, H) = \mu_\Phi^2 (\Phi^\dagger \Phi) + \lambda_\Phi (\Phi^\dagger \Phi)^2 + \lambda_1 (H^\dagger H)(\Phi^\dagger \Phi) + \lambda_2 (H^\dagger \Phi)(\Phi^\dagger H) + \frac{\lambda_3}{2} [(H^\dagger \Phi)^2 + h.c.]$$

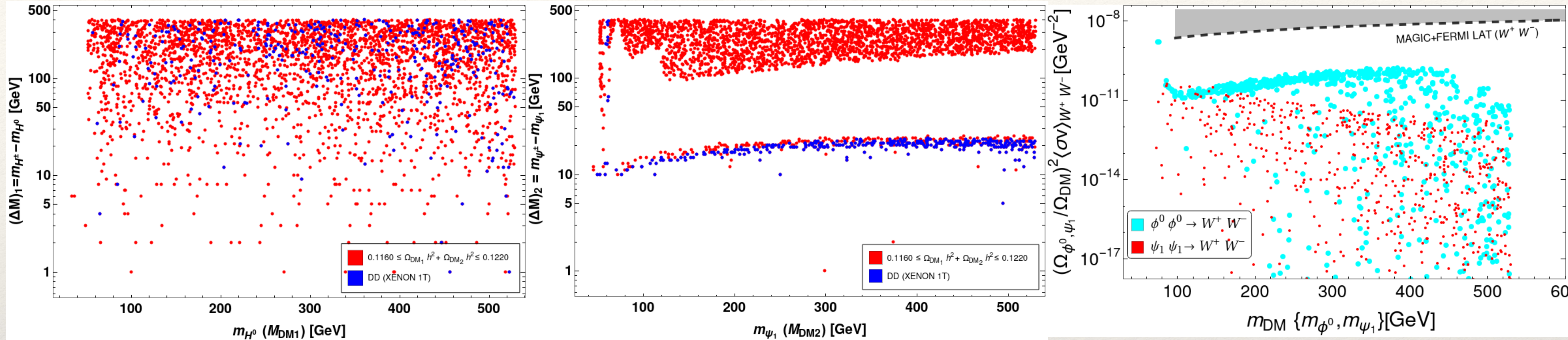
$$\{m_{\text{DM}_1},~\Delta m_1,~\lambda_L\}.$$

$$\lambda_1~=~2\lambda_L-\tfrac{2}{v^2}(m_{\phi^0}^2-m_{\phi^\pm}^2)$$

$$\begin{aligned} \mathcal{L}^{\text{FDM}} &= \overline{\Psi}_{L(R)} \left[i\gamma^\mu (\partial_\mu - ig_2 \frac{\sigma^a}{2} W_\mu^a - ig_1 \frac{Y'}{2} B_\mu) \right] \Psi_{L(R)} + \overline{\chi_R} (i\gamma^\mu \partial_\mu) \chi_R \\ &- m_\psi \overline{\Psi} \Psi - \left(\frac{1}{2} m_\chi \overline{\chi_R} (\chi_R)^c + h.c \right) - \frac{Y}{\sqrt{2}} \left(\overline{\Psi_L} \tilde{H} \chi_R + \overline{\Psi_R} \tilde{H} \chi_R^c \right) + h.c \end{aligned}$$

$$\{m_{\text{DM}_2},~\Delta m_2,~\sin\theta\};$$

DM constraints and Benchmark points

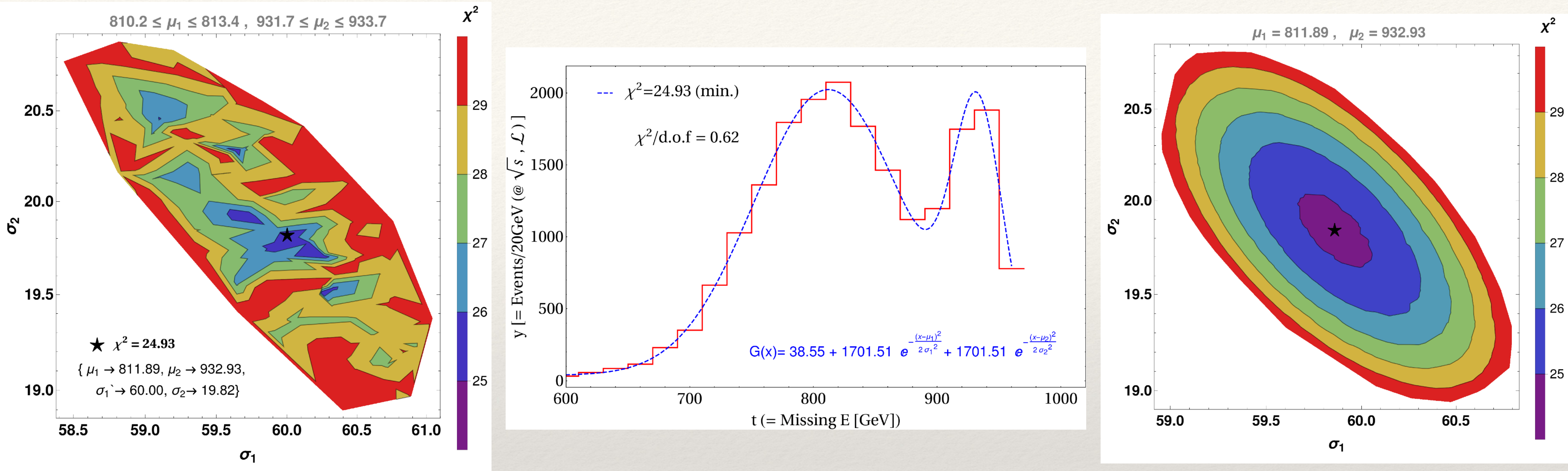


BPs	SDM sector $\{m_{\phi^0}, \Delta m_1, \lambda_L\}$	FDM sector $\{m_{\psi_1}, \Delta m_2, \sin \theta\}$	$\Omega_{\phi^0} h^2$	$\Omega_{\psi_1} h^2$	$\sigma_{\phi^0}^{\text{eff}} (\text{cm}^2)$	$\sigma_{\psi_1}^{\text{eff}} (\text{cm}^2)$	$\text{BR}(H_{\text{inv}})\%$
BP1	100, 10, 0.01	60.5, 370, 0.022	0.00221	0.1195	3.45×10^{-46}	2.03×10^{-47}	0.25
BP2	100, 10, 0.01	58.91, 285, 0.032	0.00221	0.10962	3.45×10^{-46}	5.38×10^{-47}	1.60
BP3	100, 10, 0.01	58.87, 176, 0.04	0.00221	0.11941	3.45×10^{-46}	5.00×10^{-47}	1.50
BP4	100, 10, 0.01	58.48, 190, 0.042	0.00221	0.1114	3.45×10^{-46}	7.01×10^{-47}	2.4

Benchmarks		Collider cross-section (fb)								
		$\sigma_{\text{total}}(\text{OSD})$			$\sigma_{\phi^+ \phi^-}(\text{OSD})$			$\sigma_{\psi^+ \psi^-}(\text{OSD})$		
\sqrt{s}	Points	P1	P2	P3	P1	P2	P3	P1	P2	P3
1000	BP1	232(10.8)	115(5.5)	58.5(2.75)	57.4(2.9)	28.9(1.5)	14.5(0.75)	173(8.4)	83.0(4.0)	44.0(2.0)
	BP2	276(13.4)	141(6.6)	70.0(3.3)	57.4(2.9)	28.9(1.5)	14.5(0.75)	218(10.4)	111(5.3)	55.5(2.7)
500	BP3	686(33.0)	339(15.9)	168.1(7.8)	180(8.9)	90.3(4.5)	44.3(2.3)	494(22.2)	253(11.3)	123.8(5.5)
	BP4	345(16.7)	170(8.4)	83.5(3.9)	180(8.9)	90.3(4.5)	44.3(2.3)	171.4(7.4)	82.4(3.9)	39.2(1.9)

- Higgs resonance region for FDM sector to account for DM constraints
- BP1, BP2 can be probed with 1000 GeV CM energy, BP3, BP4 at 500 GeV
- Polarisation P3 helps reducing the SM background

Gaussian Fitting



Minimize:

$$G(\mu_1, \sigma_1; \mu_2, \sigma_2) = A_1 e^{-\frac{(x-\mu_1)^2}{2\sigma_1^2}} + A_2 e^{-\frac{(x-\mu_2)^2}{2\sigma_2^2}} + \mathcal{B} .$$

$$\chi^2(\mu_1, \sigma_1; \mu_2, \sigma_2) = \sum_{i=1}^n \frac{\left(G(\mu_1, \sigma_1; \mu_2, \sigma_2)[x_H^i] - y_H^i \right)^2}{y_H^i}$$

$\chi^2/\text{d.o.f} < 1$ is statistically accurate